FULL PAPER

Dalton
www.rsc.org/dalton

Syntheses, crystal structures, photophysics and cation-binding studies of luminescent functionalized ruthenium polypyridine complexes with orthometallated aminocarbene ligands

Vivian Wing-Wah Yam,* Chi-Chiu Ko, Ben Wai-Kin Chu and Nianyong Zhu
Open Laboratory of Chemical Biology of the Institute of Molecular Technology for Drug Discovery and Synthesis, Centre for Carbon-Rich Molecular and Nano-Scale Metal-Based Materials Research, and Department of Chemistry, The University of Hong Kong, Pokfulam Road, Hong Kong SAR, People's Republic of China.
E-mail: wwyam@hku.hk; Fax: +(852)2857-1586; Tel: +(852)2859-2153

Received 30th June 2003, Accepted 8th August 2003
First published as an Advance Article on the web 3rd September 2003

A series of luminescent functionalized ruthenium polypyridine complexes with orthometallated aminocarbene ligands has been synthesized and their photophysical properties studied. The cation-binding properties of one crown-ether functionalized complexes have also been studied. The X-ray crystal structures of $[\overline{Ru(bpy)_2=C(CH_2–B15C5)NHC}_6H_3Br]OTf$ and $[\overline{Ru(5,5'\text{-}Me_2bpy)_2=C(CH_2Ph)NHC}_6H_3Br]OTf$ have been determined (bpy = 2,2′-bipyridine; 5,5′-Me_2bpy = 5,5′-dimethyl-2,2′-bipyridine; B15C5 = benzo-15-crown-5).

Introduction

Ruthenium(II) polypyridine complexes have been shown to exhibit rich photophysical and photochemical properties.[1] However, the incorporation of metal–carbon multiple-bonded ligands into the polypyridyl ruthenium systems is much less explored[2] despite the recent discovery of important catalytic properties in ruthenium–carbon multiple-bonded systems, such as ring-opening metathesis polymerization (ROMP), ring closing metathesis (RCM) and carbonylation olefination reactions in ruthenium alkylidene complexes with phosphine ligands,[3] which have attracted wide interest and enormous attention. Corresponding studies on the ruthenium alkylidene systems with N-donor ligands are relatively less explored.[4] Recently, we reported the synthesis of a new class of luminescent ruthenium(II) aminocarbene complexes with bipyridine or phenanthroline ligands.[2] Herein, as an extension of the work, we report the syntheses, crystal structures, and photophysical studies of a series of functionalized ruthenium(II) aminocarbene complexes with bipyridyl ligands. The cation-binding properties of a crown ether-containing ruthenium aminocarbene complex are also described.

Experimental

Reagents and materials

$RuCl_3·3H_2O$ was obtained from Strem Chemicals, Inc. 2,2′-Bipyridine (bpy), silver trifluoromethanesulfonate, phenylacetylene and 2-methylbut-1-en-3-yne were obtained from Aldrich Chemical Company and were used without purification. *p*-Bromoaniline was obtained from Lancaster Chemical Company and vacuum sublimed before use. Aniline was obtained from Aldrich Chemical Company and was distilled before use. 5,5′-Dimethyl-2,2′-bipyridine was prepared by palladium-catalyzed homo-coupling of 2-bromo-5-methyl-pyridine according to a literature procedure.[5] 4-Ethynylbenzo-15-crown-5 (HC≡C-B15C5)[6] and 1,4-diethynylbenzene[7] were prepared by literature procedures. The ruthenium(II) starting materials, *cis*-$[Ru(bpy)_2Cl_2]$ and *cis*-$[Ru(5,5'\text{-}Me_2bpy)_2Cl_2]$, were prepared according to literature methods[8] but with DMF as the solvent instead of ethylene glycol. $[\overline{Ru(bpy)_2=C(CH_2Ph)NHC}_6H_3Br]PF_6$ (**1**) and $[\overline{Ru(bpy)_2=C(CH_2Ph)NHC}_6H_3CF_3]PF_6$ (**2**) were prepared as reported previously.[2b] Acetone (Merck, GR) was distilled over anhydrous magnesium sulfate before use. Acetonitrile (Lab-Scan, AR) was used as obtained for synthesis and distilled over calcium hydride for physical measurements. All other reagents were of analytical grade and were used as received.

Syntheses

All reactions were performed under strictly anaerobic and anhydrous conditions in an inert atmosphere of nitrogen using standard Schlenk technique.

$[\{\overline{Ru(bpy)_2=C(NHC}_6H_4)CH_2\}_2C_6H_4](OTf)_2$, 3. The title complex was synthesized by modification of a procedure reported previously.[2] *Cis*-$[Ru(bpy)_2Cl_2]·2H_2O$ (100 mg, 0.19 mmol) and AgOTf (100 mg, 0.39 mmol) were mixed and stirred in anhydrous acetone (20 ml) for 3 hours. The solution was filtered to remove the precipitated AgCl and was evaporated to dryness under reduced pressure. Reaction of *cis*-$[Ru(bpy)_2(Me_2CO)_2](OTf)_2$ with 1,4-diethynylbenzene (12 mg, 0.1 mmol) in the presence of an excess of aniline (72 mg, 0.77 mmol) in anhydrous acetone gave a purple solution. This was filtered and evaporated to dryness under reduced pressure. The purple residue was then washed with diethyl ether (4 × 7 ml). Subsequent recrystallization by slow diffusion of diethyl ether vapour into a concentrated DMF solution of the complex yielded purple micro-crystals. Yield: 108 mg, 0.076 mmol; 40%. ^{1}H NMR (300 MHz, CD_3CN, 298 K): δ 4.0 (d, J = 8 Hz, 4H, CH_2), 5.5 (s, 4H, aromatic H), 6.3 (d, J = 12 Hz, 2H, aromatic H), 6.6 (t, J = 7 Hz, 2H, aromatic H), 6.8 (t, J = 8 Hz, 2H, aromatic H), 7.1 (t, J = 8 Hz, 2H, aromatic H), 7.2–8.3 (m, 32 H, aromatic H), 11.1 (s, 2H, aromatic H). Positive ESI-MS: *m*/*z* 1287 $\{M - OTf\}^+$, 570 $\{M\}^{2+}$. Elemental analyses, Found (%): C 51.26, H 3.49, N 9.22; Calcd. for **2**·¼DMF (%): C 51.47, H 3.45, N 9.27.

$[\overline{Ru(5,5'\text{-}Me_2bpy)_2=C(CH_2Ph)NHC}_6H_3Br]OTf$, 4. The title complex was synthesized according to a procedure similar to that of **1** except *cis*-$[Ru(5,5'\text{-}Me_2bpy)_2Cl_2]·2H_2O$ (112 mg, 0.19 mmol) was used in place of *cis*-$[Ru(bpy)_2Cl_2]·2H_2O$. Slow diffusion of diethyl ether vapor into a concentrated acetonitrile solution of the complex gave **2**, isolated as brown crystals. Yield: 152 mg, 0.17 mmol; 90%. ^{1}H NMR (500 MHz, CD_3CN, 298 K): δ 4.22 (m, 2H, CH_2–C=Ru), 6.31 (d, 2H, J = 7.5 Hz, aromatic H), 6.42 (s, 1H, aromatic H), 6.74–6.77 (m, 2H, aromatic H), 6.90–6.94 (m, 2H, aromatic H), 7.06 (s, 1H, aromatic H), 7.17 (d, 1H, J = 8.1 Hz, aromatic H), 7.45 (s, 1H, aromatic H), 7.49–

DOI: 10.1039/b307429c

7.61 (m, 4H, aromatic H), 7.69 (d, 2H, J = 8.3 Hz, aromatic H), 7.76 (d, 1H, J = 8.1 Hz, aromatic H), 7.82 (s, 1H, aromatic H), 8.06 (d, 1H, J = 7.5 Hz, aromatic H), 8.15 (d, 1H, J = 7.5 Hz, aromatic H), 11.20 (s, broad, 1H, NH). ^{13}C NMR (125.8 MHz, CD_3CN, 298 K): δ 52.5 (CH_2), 115.4–182.6 (aromatic C), 266.1 (Ru=C). Positive ESI-MS: m/z 744 {M − OTf}$^+$. Elemental analyses, Found (%): C 52.53, H 4.02, N 7.54; Calcd. for **2** (%): C 52.53, H 3.95, N 7.85.

[Ru(bpy)$_2$=C(CH$_2$C(CH$_3$)=CH$_2$)NHC$_6$H$_3$Br]OTf, 5. The title complex was synthesized according to a procedure similar to that of **1** except 2-methylbut-1-en-3-yne (38 mg, 0.58 mmol) was used in place of phenylacetylene. Slow diffusion of diethyl ether vapor into a concentrated acetonitrile solution of the complex gave **3**, isolated as purple crystals. Yield: 72 mg, 0.09 mmol; 45%. ^{1}H NMR (300 MHz, CD_3CN, 298 K): δ1.14 (s, 3H, –Me), 3.66 (d, 1H, J = 14.4 Hz, –C=CH$_2$), 3.74 (d, 1H, J = 14.4 Hz, –C=CH$_2$), 4.42 (m, 2H, CH$_2$–C=Ru), 6.54 (d, 1H, J = 2.2 Hz, aromatic H), 7.05 (d, 1H, J = 8.1 Hz, aromatic H), 7.28 (d, 1H, J = 8.1 Hz, aromatic H), 7.34–7.59 (m, 5H, aromatic H), 7.89–8.16 (m, 7H, aromatic H), 8.38–8.49 (m, 4H, aromatic H), 11.2 (s, broad, 1H, NH). ^{13}C NMR (75.5 MHz, CD_3CN, 298 K): δ21.9 (CH_3), 53.5 (CH_2), 114.2–183.0 (aromatic C), 267.4 (Ru=C). Positive ESI-MS: m/z 650 {M − OTf}$^+$. Elemental analyses, Found (%): C 48.45, H 3.38, N 8.72; Calcd. for **3** (%): C 48.06, H 3.40, N 8.76.

[Ru(bpy)$_2$=C(CH$_2$B15C5)NHC$_6$H$_3$Br]OTf, 6. The title complex was synthesized according to a procedure similar to that of **1** except HC≡C-B15C5 (60 mg, 0.2 mmol) was used in place of phenylacetylene. Slow diffusion of diethyl ether vapor into a concentrated methanol–dichloromethane solution of the complex gave **4**, isolated as purple crystals. Yield: 112 mg, 0.11 mmol; 55%. ^{1}H NMR (300 MHz, CD_3CN, 298 K): δ3.52–3.59 (m, 12H, –OCH$_2$CH$_2$O–), 3.64–3.67 (m, 2H, C$_6$H$_3$–CH_2O–), 3.81–3.84 (m, 2H, C$_6$H$_3$–CH_2O–), 4.07 (s, 2H, CH$_2$–C=Ru), 5.55 (dd, 1H, J = 8.0 Hz, 1.9 Hz, aromatic H of crown ether moiety), 5.70 (d, 1H, J = 1.9 Hz, aromatic H of crown ether moiety), 6.10 (d, 1H, J = 8.0 Hz, aromatic H of crown ether moiety), 6.83–6.85 (m, 1H, aromatic H), 7.06–7.22 (m, 6H, aromatic H), 7.56–7.86 (m, 9H, aromatic H), 8.04 (d, 1H, J = 7.5 Hz, aromatic H), 8.15 (d, 1H, J = 8.3 Hz, aromatic H), 8.22 (d, 1H, J = 7.5 Hz, aromatic H), 11.1 (s, broad, 1H, NH). ^{13}C NMR (75.5 MHz, CD_3CN, 298 K): δ 52.2 (CH_2), 68.6–71.4 (O–CH$_2$CH$_2$–O), 113.9–182.1 (aromatic C), 267.7 (Ru=C). Positive ESI-MS: m/z 878 {M − OTf}$^+$. Elemental analyses, Found (%): C 48.97, H 4.06, N 6.51; Calcd. for **4**·CH$_2$Cl$_2$ (%): C 48.91, H 3.96, N 6.55.

Physical measurements and instrumentation

^{1}H and ^{13}C NMR spectra were recorded on either a Bruker DPX-300 (300 MHz) or a Bruker DRX-500 (500 MHz) FT-NMR spectrometer. Chemical shifts were recorded relative to tetramethylsilane (Me_4Si). Positive-ion FAB mass spectra were recorded on a Finnigan MAT95 mass spectrometer. Electrospray-ionization mass spectra were recorded on a Finnigan LCQ mass spectrometer. Elemental analyses of all the metal complexes were performed on a Carlo Erba 1106 elemental analyzer by the Institute of Chemistry at the Chinese Academy of Sciences in Beijing.

Electronic absorption spectra were recorded on a Hewlett-Packard 8452A diode array spectrophotometer. Steady state emission and excitation spectra at room temperature and 77 K were recorded on a Spex Fluorolog-2 Model F 111 fluorescence spectrophotometer. Solid state photophysical measurements were carried out with solid samples contained in a quartz tube inside a quartz-walled Dewar flask. Measurements of the EtOH–MeOH (4 : 1, v/v) glass or solid state samples at 77 K were similarly conducted with liquid nitrogen filled in the optical Dewar flask. Excited state lifetimes of solid and solution samples were measured using a conventional laser system. The excitation source was the 355-nm output (third harmonic, 8 ns) of a Spectra-Physics Quanta-Ray Q-switched GCR-150 pulsed Nd-YAG laser (10 Hz). Luminescence decay traces were recorded on a Tektronix Model TDS 620A digital oscilloscope and the lifetime (τ) determination was accomplished by the single exponential fitting of the luminescence decay traces with the model, $I(t) = I_0 \exp(-t/\tau)$, where $I(t)$ and I_0 stand for the luminescence intensity at time = t and time = 0, respectively. Solution samples for photophysical measurements were degassed with no less than four freeze–pump–thaw cycles.

The electronic absorption spectral titration experiments for binding constant determination were performed with a Hewlett-Packard 8452A diode array spectrophotometer at 25 °C, which was controlled by a Lauda RM6 compact low-temperature thermostat. Supporting electrolyte (0.1 mol dm^{-3} ^{n}Bu$_4$NPF$_6$) was added to maintain a constant ionic strength of the sample solution in order to avoid any changes arising from a change in the ionic strength of the medium. Binding constants for 1 : 1 complexation were obtained by a non-linear least-squares fit[9] of the absorbance (A) *versus* the concentration of the metal ion added ([M^{n+}]) according to the following equation:

$$A = A_0 + \frac{A_\infty - A_0}{2[\mathrm{Ru}]}\left([\mathrm{Ru}] + [\mathrm{M}^{n+}] + \frac{1}{K_s} - \sqrt{([\mathrm{Ru}] + [\mathrm{M}^{n+}] + \frac{1}{K_s})^2 - 4[\mathrm{Ru}][\mathrm{M}^{n+}]}\right)$$

where A_0 and A are the absorbance of the complex at a selected wavelength in the absence and presence of the metal cation, respectively, [Ru] is the total concentration of the crown ether-containing ruthenium(II) complex, [M^{n+}] is the concentration of the metal cation M^{n+}, A_∞ is the limiting value of absorbance in the presence of a large excess of metal ion and K_s is the stability constant.

Crystal structure determination

Experimental details for the crystal structure determinations are summarized in Table 1. Crystals of **4** suitable for X-ray diffraction studies were obtained by slow diffusion of diethyl ether vapor into a concentrated acetonitrile solution of **4**. A dark brown crystal mounted in a glass capillary was used for data collection at −20 °C on a MAR diffractometer with a 300 mm image plate detector using graphite monochromatized Mo-Kα radiation (λ = 0.71073 Å). Data collections were made with 2° oscillation of φ, 420 seconds exposure time and scanner distance at 120 mm. 90 images were collected and interpreted, and intensities were integrated using the program *DENZO*.[10] The structure was solved by direct methods employing the *SIR-97* program[11] on a PC. The Ru, Br and many atoms were located according to the direct methods. The positions of the other atoms were found after successful refinement by full-matrix least-squares using program *SHELXL-97*[12] on a PC. One crystallographic asymmetric unit consisted of one formula unit, *i.e.* a complex cation and one $CF_3SO_3^-$ anion. In the final stage of least-squares refinement, all the other non-hydrogen atoms were refined anisotropically. H atoms were generated by program *SHELXL-97*.[12] The positions of H atoms were calculated based on riding mode with thermal parameters equal to 1.2 times that of the associated C atoms, and participated in the calculation of final R-indices. The final difference Fourier map was featureless.

Crystals of **6** suitable for X-ray diffraction studies were obtained by slow diffusion of diethyl ether vapor into a concentrated acetonitrile solution of **6**. A purple crystal mounted in a glass capillary was used for data collection at 28 °C on a MAR

Table 1 Crystal and structure determination data for complexes **4** and **6**

Compound	**4**	**6**
Formula	$[C_{38}H_{35}BrN_5Ru]^+ (CF_3SO_3^-)$	$[C_{42}H_{41}BrN_5O_5Ru]^+ (CF_3SO_3^-)\cdot(CH_3CH_2)_2O$
M_r	891.76	1099.97
T/K	253	301
a/Å	10.536(2)	14.063(3)
b/Å	13.332(3)	17.027(3)
c/Å	14.986(3)	20.484(4)
α/°	69.68(3)	90
β/°	82.28(3)	91.50(3)
γ/°	74.50(3)	90
V/Å^3	1900.2(7)	4903.2(17)
Crystal colour	Dark brown	Purple
Crystal system	Triclinic	Monoclinic
Space group	$P\bar{1}$	$P2_1/n$
Z	2	4
F(000)	900	2248
D_c/g cm^{-3}	1.559	1.490
Crystal dimensions/mm	0.30 × 0.30 × 0.20	0.50 × 0.10 × 0.10
λ/Å (graphite monochromated, Mo-Kα)	0.71073	0.71073
μ/cm^{-1}	15.78	12.47
Oscillation/°	2	2
No. of images collected	90	61
Distance/mm	120	120
Exposure time/s	420	300
No. of data collected	8494	13983
No. of unique data	4807	6405
No. of data used in refinement, m	3416	3926
No. of parameters refined, p	486	604
R^a	0.0431	0.0452
wR^a	0.1092	0.1116
Residual extrema in final difference map/e Å^{-3}	+1.171, −0.434	+0.535, −0.382

[a] $w = 1/[\sigma^2(F_o^2)+(aP)^2+bP]$, where $P = [2F_c^2\mathrm{Max}(F_o^2,0)]/3$.

diffractometer with a 300 mm image plate detector using graphite monochromatized Mo-Kα radiation (λ = 0.71073 Å). Data collections were made with 2° oscillation of φ, 300 seconds exposure time and scanner distance at 120 mm. 61 images were collected and interpreted, and intensities were integrated using the program *DENZO*.[10] The structure was solved by direct methods employing the *SHELXS-97* program[12] on a PC. The Ru, Br and many atoms were located according to the direct methods. The positions of the other non-hydrogen atoms were found after successful refinement by full-matrix least-squares using program *SHELXL-97*[12] on a PC. One crystallographic asymmetric unit consisted of one formula unit, *i.e.* a complex cation, one $CF_3SO_3^-$ anion and one solvent molecule of Et_2O. In the final stage of least-squares refinement, all the other non-hydrogen atoms were refined anisotropically. H atoms on the non-disordered atoms were generated by program *SHELXL-97*.[12] The positions of H atoms were calculated based on riding mode with thermal parameters equal to 1.2 times that of the associated C atoms, and participated in the calculation of final *R*-indices. The final difference Fourier map was featureless.

CCDC reference numbers 213863 and 213864.

See http://www.rsc.org/suppdata/dt/b3/b307429c/ for crystallographic data in CIF or other electronic format.

Results and discussion

Synthesis and characterization

The synthetic route employed, as shown in Scheme 1, for the preparation of the ruthenium(II) orthometallated aminocarbene complexes was similar to that reported previously.[2] In the presence of anilines, the ruthenium(II) vinylidene complexes, which are initially formed by the reaction of the terminal acetylenes with the coordinatively unsaturated ruthenium starting complexes, react with anilines in anhydrous acetone to give the orthometallated aminocarbene complexes. A wide variety of anilines, ranging from the electron-deficient trifluoromethyl- to the electron-rich methoxy- substituted anilines, have been employed in the synthesis of the ruthenium(II) aminocarbene complexes. Of the various anilines employed in these syntheses, *p*-bromoaniline gave the highest yield of the ruthenium aminocarbene complexes formed, with almost quantitative production. The *p*-bromoaniline was also found to be the most versatile of all nucleophiles used for this reaction. As a result, the reaction with the use of *p*-bromoaniline was found to be successful with most acetylenes used, including ethynylbenzo-15-crown-5 and 2-methylbut-1-en-3-yne, while with the other anilines the reactions only gave very low to almost no yield. In addition, ruthenium(II) aminocarbene complexes with different diimine ligands, such as 5,5′-dimethyl-2,2′-bipyridine, have also been synthesized under similar reaction conditions by using the respective $[Ru(N–N)_2Cl_2]$ as the starting material. The identities of the complexes have been confirmed by satisfactory elemental analyses, ^{1}H and ^{13}C NMR spectroscopies and FAB mass spectrometry. Complexes **4** and **6** have also been characterized by X-ray crystallography.

X-Ray crystal structures

Fig. 1 and 2 depict the perspective drawings of the complex cations of **4** and **6**, respectively. The crystal and structure determination data and the selected bond distances and bond angles are summarized in Tables 1 and 2, respectively. The N–Ru–N bond angles subtended by the chelating bipyridine ligands in **4** and **6** are in the range of 76.8 and 77.9°. The relatively large deviation from an ideal 90° for a regular octahedral geometry is a result of the steric requirement of the bidentate ligands. The bond angles of the orthometallated aminocarbene ligand, C–Ru–C, for **4** and **6** are 79.6 and 80.1°, respectively, which are comparable to those found in other orthometallated carbene complexes.[13] The bond angles around the carbene carbon range from 113.5 to 130.0°, which are consistent with the sp^2 hybridization of the carbene carbon. The Ru–N bonds (2.050–2.060 Å) that are *trans* to the pyridine rings have similar bond lengths as those found in other ruthenium(II) polypyridyl complexes (*ca.* 2.05 Å),[14] but those *trans* to the orthometallated

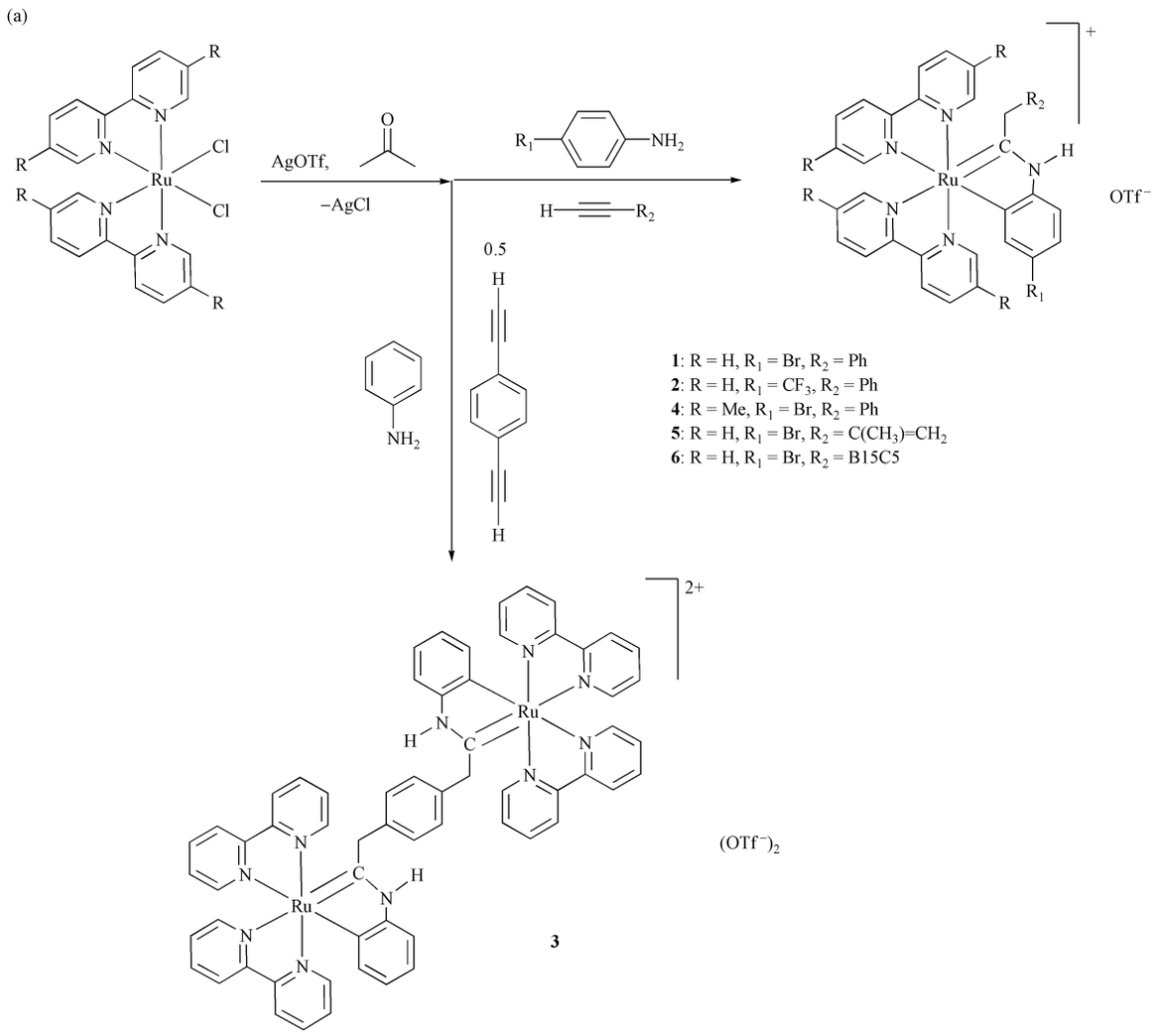

Scheme 1 General synthetic route for ruthenium(II) orthometallated aminocarbene complexes.

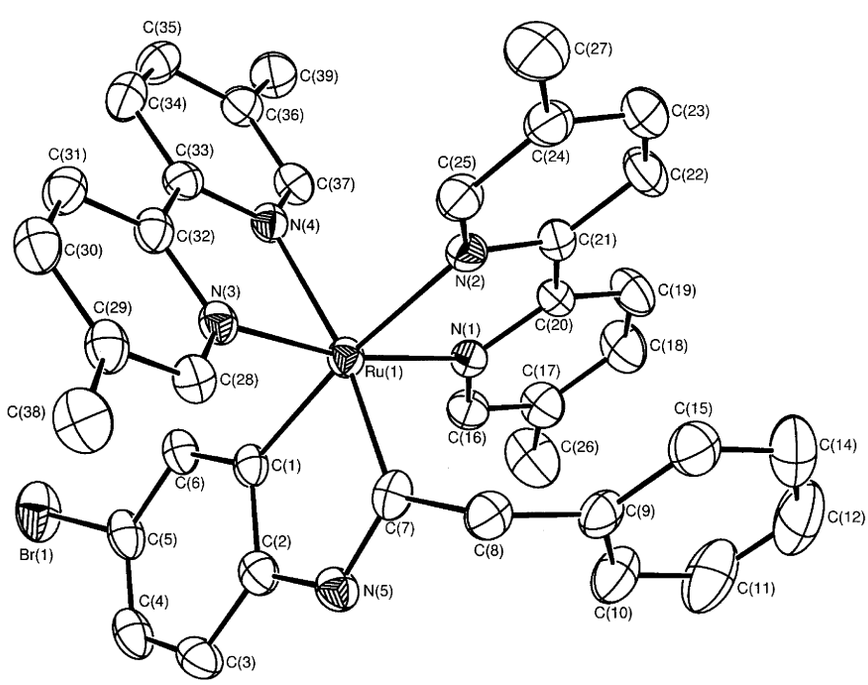

Fig. 1 Perspective drawing of the complex cation of **4** with the atomic numbering scheme. Hydrogen atoms have been omitted for clarity. Thermal ellipsoids are shown at the 30% probability level.

and the carbene carbon atoms (2.129–2.152 Å) are much longer than normal. This may be due to the stronger *trans* influence of the orthometallated and the carbene carbon atoms compared to the nitrogen atoms in bipyridine. The two Ru–C(sp^2) distances for the orthometallated and the carbene carbons are quite different. The Ru–C(carbene) bond distances, 1.952 Å for

Table 2 Selected bond distances (Å) and angles (°) with estimated standard deviations (e.s.d.s) in parentheses for **4** and **6**

4	Ru(1)–C(7)	1.952(6)	Ru(1)–N(1)	2.064(5)
	Ru(1)–C(1)	2.050(5)	Ru(1)–N(2)	2.136(4)
	Ru(1)–N(3)	2.060(5)	Ru(1)–N(4)	2.151(5)
	C(7)–C(8)	1.512(8)	N(5)–C(7)	1.336(7)
	N(1)–Ru(1)–N(2)	77.20(18)	N(3)–Ru(1)–N(4)	77.87(19)
	C(7)–Ru(1)–C(1)	79.6(2)	N(5)–C(7)–Ru(1)	117.3(4)
	N(5)–C(7)–C(8)	114.2(5)	C(8)–C(7)–Ru(1)	128.5(5)
6	Ru(1)–C(27)	1.963(6)	Ru(1)–N(1)	2.060(5)
	Ru(1)–C(21)	2.020(6)	Ru(1)–N(2)	2.129(5)
	Ru(1)–N(3)	2.055(4)	Ru(1)–N(4)	2.141(5)
	C(27)–C(28)	1.521(7)	N(5)–C(27)	1.338(7)
	N(1)–Ru(1)–N(2)	77.2(2)	N(3)–Ru(1)–N(4)	76.88(18)
	C(27)–Ru(1)–C(21)	80.1(2)	C(28)–C(27)–Ru(1)	130.0(4)
	N(5)–C(27)–C(28)	113.5(5)	N(5)–C(27)–Ru(1)	116.5(4)

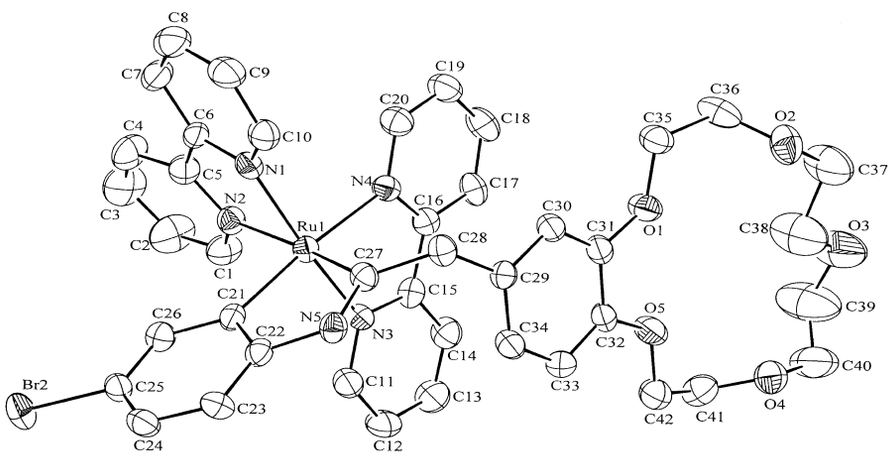

Fig. 2 Perspective drawing of the complex cation of **6** with the atomic numbering scheme. Hydrogen atoms have been omitted for clarity. Thermal ellipsoids are shown at the 30% probability level.

4 and 1.963 Å for **6**, are much shorter than those, 2.050 Å for **4** and 2.020 Å for **6**, of the Ru–C(orthometallated phenyl carbon). This is ascribed to the presence of the double bond character in the ruthenium–carbene carbon bonds. The carbene carbon–nitrogen bond distances, 1.336 Å for **4** and 1.338 Å for **6**, are shorter than that of a typical C–N (sp^2) bond, which is characteristic of Fischer type aminocarbenes (*ca.* 1.31 Å).[15] The shortening of the C–N bond is attributed to a substantial double bond character between the nitrogen and the carbene carbon, resulting from the π-delocalization of the lone pair electron on nitrogen and is typically observed in the Fischer type aminocarbenes.[15]

Electronic absorption and emission properties

The electronic absorption spectra show intense absorption bands at *ca.* 250, 298 and 368 nm in the UV region, with molar extinction coefficients in the order of 10^4 dm^3 mol^{-1} cm^{-1}, which are ascribed to the intraligand π ⟶ π* transitions of the bipyridine and orthometallated amino-carbene ligands. Two additional moderately intense bands, with molar extinction coefficients in the order of 10^3 dm^3 mol^{-1} cm^{-1}, at *ca.* 460–490 nm and 536–554 nm are assigned as metal-to-ligand charge transfer (MLCT) transitions of Ru(dπ) ⟶ π*(carbene) and Ru(dπ) ⟶ π*(bpy) respectively, probably with some mixing of a ligand-to-ligand charge transfer (LLCT) [π(aminocarbene) ⟶ π*(bpy)] transition. The electronic absorption data for complexes **1**–**6** are summarized in Table 3. The absorption energies of both bands are in the order of **4** (460, 536 nm) > **2** (464, 548 nm) > **1** (470, 554 nm) ≈ **6** (470, 554 nm) ≈ **5** (472, 556 nm) > **3** (480, 570 nm), which is in agreement with an MLCT assignment of Ru(dπ) ⟶ π*(carbene) and Ru(dπ) ⟶ π*(bpy) in nature. In general, the presence of electron-releasing substituents on the bpy and carbene ligands would raise the π* orbital energies of the respective ligands, leading to a higher MLCT energy, whereas with electron-withdrawing substituents on the bpy and carbene ligands, the converse is true. The relatively lower energy band is tentatively assigned as the MLCT transition of Ru(dπ) ⟶ π*(bpy) as it is more sensitive to the nature of the diimine ligand and the π* orbital of bpy is believed to be lower-lying in energy than that of the carbene ligand, as supported by EHMO calculations.[2b]

Upon excitation at $\lambda > 350$ nm, complexes **1**–**6** in acetonitrile solution display red luminescence with emission maxima in the range of 755–813 nm. Fig. 3–4 show the representative emission spectra of selected complexes. The emission energies, as reflected from the emission maxima, are in the order of **4** (755 nm) >> **1** (792 nm) and **2** (782 nm) > **1** (792 nm) ≈ **5** (792 nm) ≈

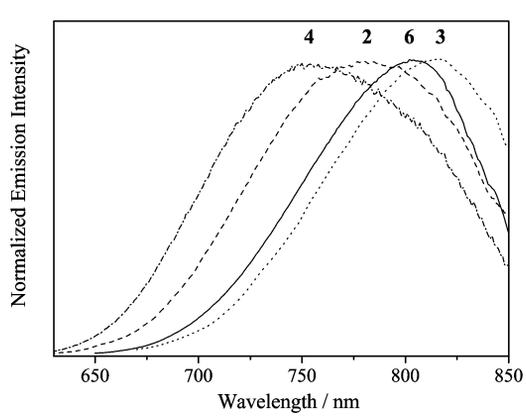

Fig. 3 Overlaid corrected emission spectra of selected complexes in acetonitrile solution at 298 K.

Table 3 Photophysical data for complexes **1**–**6**

Complex	Medium (*T*/K)	Emission λ_{em}[a]/nm (τ_0/μs)	Absorption λ_{abs}[b]/nm (ε/dm^3 mol^{-1} cm^{-1})
1[c]	MeCN (298)	792 (<0.1)	250 (36300), 296 (45300), 366 (11390), 470 (6610), 554 (6960)
	Solid (298)	754	
	Solid (77)	685	
	Glass[d] (77)	706	
2[c]	MeCN (298)	782 (<0.1)	248 (36870), 296 (42410), 368 (9960), 464 (5740), 548 (6140)
	Solid (298)	740	
	Solid (77)	700	
	Glass[d] (77)	700	
3	MeCN (298)	810 (<0.1)	286 (64210), 296 (72935), 370 (21295), 480 (11360), 570 (13320)
	Solid (298)	789	
	Solid (77)	737	
	Glass[d] (77)	748	
4	MeCN (298)	755 (<0.1)	256 (48120), 304 (55580), 370 (10920), 460 (7090), 536 (7460)
	Solid (298)	720	
	Solid (77)	687	
	Glass[d] (77)	688	
5	MeCN (298)	792 (<0.1)	248 (34790), 296 (47240), 366 (11640), 472 (6660), 556 (6700)
	Solid (298)	750	
	Solid (77)	688	
	Glass[d] (77)	708	
6	MeCN (298)	794 (<0.1)	248 (29420), 288 (33450), 296 (37580), 366 (9350), 470 (5320), 554 (5800)
	Solid (298)	755	
	Solid (77)	688	
	Glass[d] (77)	708	

[a] Excitation wavelength at 580 nm. Emission maxima are corrected values. [b] In acetonitrile at 298 K. [c] Data obtained from reference 2*b*. [d] EtOH–MeOH (4 : 1 v/v).

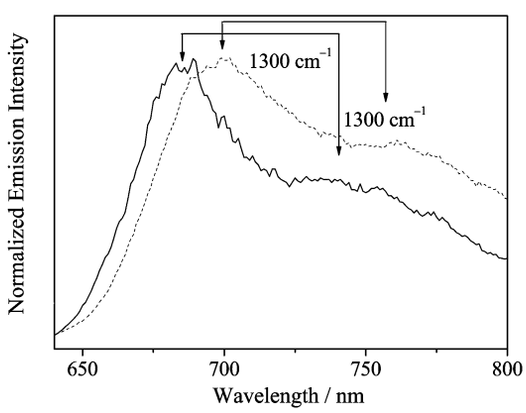

Fig. 4 Overlaid corrected emission spectra of complexes **2** (- - -) and **4** (—) in EtOH–MeOH (4 : 1 v/v) glass at 77 K.

6 (794 nm) > **3** (809 nm), which are suggestive of an assignment of a ^{3}MLCT [dπ(Ru) ⟶ π*(bpy)] origin. The emission energy is found to be sensitive to the nature of the diimine ligand, as reflected by the change in emission energies from **1** to **4** upon a change in the diimine ligand. The blue shift in emission energy of **4** relative to **1** could be explained by the presence of electron-donating methyl substituents on the bipyridine ligands, which would render the π* orbital of the diimine ligand higher-lying in energy and thus resulting in a higher MLCT emission energy. On the contrary, an assignment of a MLCT [dπ(Ru) ⟶ π*(carbene)] origin would give rise to an opposite trend, in which a higher-lying dπ(Ru) orbital energy would be expected for **4** than **1**, leading to a smaller MLCT [dπ(Ru) ⟶ π*(carbene)] emission energy for **4**. Thus an assignment of a ^{3}MLCT [dπ(Ru) ⟶ π*(carbene)] origin is disfavored. With the same diimine ligand, a relatively small emission energy dependence in the order of **2** (782 nm) > **1** (792 nm) ≈ **5** (792 nm) ≈ **6** (794 nm) > **3** (809 nm) was observed. These emission energies are in line with the electronic effect of the substituents R_1 on the orthometallated phenyl ring, in which the electron-withdrawing abilities are in the order: CF_3 > Br > H. The presence of a more electron-withdrawing substituent R_1 on the orthometallated phenyl ring would render the ruthenium metal centre less electron rich, which results in a lower-lying dπ(Ru) orbital and hence a higher MLCT emission energy. On the contrary, with the same substituent, R_1 = Br on the orthometallated phenyl ring in complexes **1**, **5** and **6**, the emission energies are insensitive to the alteration of the substitutent, R_2 ($R_2 = C_6H_5$, B15C5, $C(CH_3)=CH_2$). The insensitivity of the emission energies upon variation of the substitutents R_2 is probably attributed to the presence of the methylene spacer between R_2 and the phenyl ring, which would render the direct electronic communication between the carbene carbon and the R_2 group insignificant. An assignment of a LLCT [π(carbene) ⟶ π*(bpy)] emission origin could not be totally excluded since both MLCT [dπ(Ru) ⟶ π*(bpy)] and LLCT [π(carbene) ⟶ π*(bpy)] origins would give rise to a similar emission energy trend. However, with reference to previous spectroscopic studies on related polypyridyl ruthenium(II) complexes[16] as well as EHMO studies,[2b] an assignment of the emissions as a MLCT [dπ(Ru) ⟶ π*(bpy)] origin is more likely. In addition, some emission spectra in EtOH–MeOH (4 : 1 v/v) glass at 77 K show fairly well resolved vibronic structures with vibrational progressional spacings (ν_M) of *ca.* 1300 cm^{-1} (Fig. 4), which are typical of ν(C⋯N) stretching modes of the bpy ligands, and are commonly observed in ruthenium(II) polypyridyl complexes.[16,17] This is further supportive of an assignment of the MLCT [dπ(Ru)⟶π*(bpy)] emission origin.

Cation-binding properties of 6

The benzo-15-crown-5-containing carbene complex, **6** shows an observable UV-visible spectral change upon addition of alkali metal cations, Na^+ and Li^+. Fig. 5 shows the UV-Vis absorption spectral traces of **6** upon addition of sodium perchlorate with well defined isosbestic points. The insert shows the plot of absorbance at λ = 236 nm *versus* the concentration of metal ion and the theoretical non-linear least-squares fit. The close resemblance of the experimental data to the theoretical fit is supportive of a 1 : 1 complexation model.

The observed spectral change is mainly localized in the UV region at *ca.* 220–260 nm, with very small changes in the absorption bands in the visible region, which are assigned to the electronic transitions of dπ(Ru) ⟶ π*(carbene) and dπ(Ru) ⟶ π*(bpy). The maximum spectral changes at *ca.* 220–260 nm are probably derived from the π ⟶ π* or n ⟶ π* transitions of the

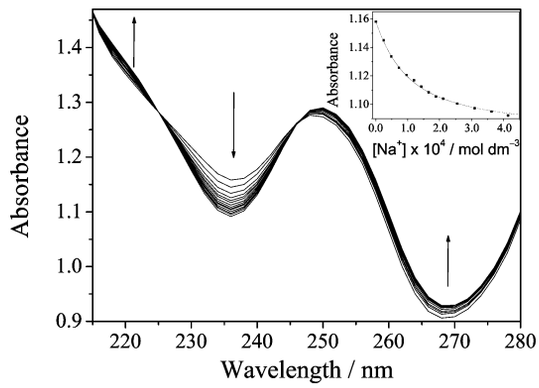

Fig. 5 Electronic absorption spectral traces of **6** in acetonitrile (0.1 mol dm^{-3} $^{n}Bu_4NPF_6$) upon addition of $NaClO_4$. The insert shows a plot of absorbance at 236 nm (■) *versus* [Na^+] and its theoretical non-linear least-squares fit (—).

crown ether moiety, and thus the perturbation is greatest upon binding of the cation in the crown ether cavity. The relatively small spectral changes observed in the visible region may be a result of the presence of the CH_2 connector, which blocks the direct electronic communication between the crown ether moiety and the ruthenium metal centre as well as the aminocarbene ligand. The complex shows very small to almost no observable UV-visible spectral changes upon addition of potassium salts. This may be due to the small cavity size of the benzo-15-crown-5 (1.70–2.20 Å),[18] which is insufficient for the binding of the potassium ion (2.66 Å).[18] Although benzo-15-crown-5 units are known to bind potassium ion in a 2 : 1 sandwich fashion,[18c] the coordination of one potassium ion to two molecules of **6** is unlikely for steric reasons. The slightly higher binding constant for the sodium ion (log $K = 4.09 \pm 0.02$) than that for the lithium ion (log $K = 4.04 \pm 0.02$) is consistent with the better size match between the sodium ion (1.94 Å)[18] and the benzo-15-crown-5 cavity (1.70–2.20 Å)[18] compared to that of the lithium ion (1.36 Å).[18] Thus, the complexation of the crown ether with the Na^+ ion would be anticipated to be stronger than that with the Li^+ ion, and hence a higher stability constant (log K) for the Na^+ ion is expected. However the higher charge density of the Li^+ ion would enhance its binding to the crown ether. As a result of these effects, the stability constant for the Na^+ ion is only very slightly higher than that for the Li^+ ion. Similar changes in the emission spectra were not observed upon metal ion-binding.

Positive ESI-mass spectrometry provides another piece of evidence for the ion-binding properties of the complexes. Positive ESI-mass spectra showing the expanded ion cluster and the simulated ion cluster of the ion-bound adduct of **6**·$NaClO_4$ are depicted in Fig. 6. A 1 : 1 adduct was observed upon addition of $NaClO_4$, $LiClO_4$ and $KClO_4$ to **6**. This further confirms the 1 : 1 complexation stoichiometry obtained from the electronic absorption studies for the Na^+ and the Li^+ ion. However, the intensity of the ion-bound species, $[M+KClO_4]^+$, is very much lower than that of $[M+NaClO_4]^+$ and $[M+LiClO_4]^+$. This is consistent with the much lower binding affinity between the K^+ ion and the benzo-15-crown-5, as reflected by electronic absorption spectral titration studies.

Conclusion

A new series of ruthenium polypyridine complexes with functionalized aminocarbene ligands was synthesized and their photophysical properties studied. With the variation of the substituents on the aminocarbene and the bipyridyl ligands, both the absorption and emission energy could be tuned and the emission origin has been elucidated to be derived from the MLCT [dπ(Ru) ⟶ π*(bpy)] phosphorescence. The cation-binding properties of the benzo-15-crown-5-containing

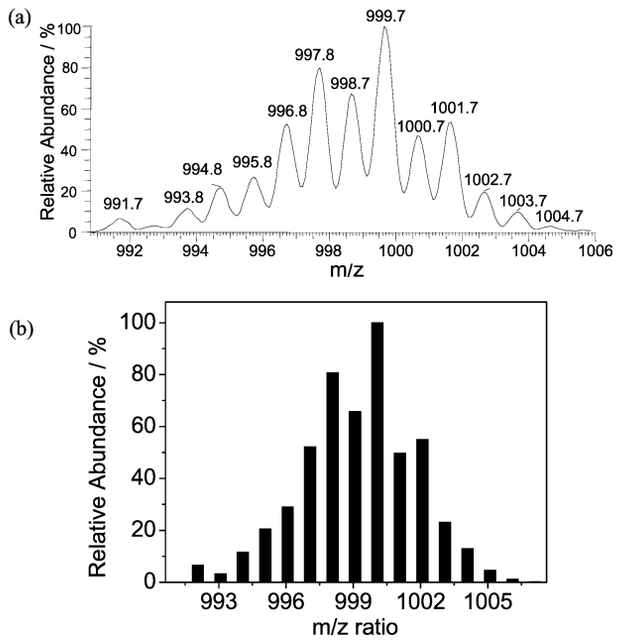

Fig. 6 Expanded ion cluster from the positive ESI-mass spectrum of an acetonitrile solution of **6** showing (a) 1 : 1 ion-bound adducts with $NaClO_4$, $[\mathbf{6}\cdot NaClO_4]^+$ at *m/z* 984 and (b) simulated isotope pattern for $[\mathbf{6}\cdot NaClO_4]^+$.

ruthenium carbene complex were studied by UV-Vis spectrophotometric methods, and confirmed by ESI-mass spectrometric studies. The binding constants (log K) for Li^+ and Na^+ ions were determined.

Acknowledgements

V. W.-W. Y. acknowledges support from The University of Hong Kong Foundation for Educational Development and Research Limited and the University Grants Committee Area of Excellence Scheme, C.-C. K. the receipt of a Croucher Scholarship from Croucher Foundation and Li Po Chun Postgraduate Scholarship from Li Po Chun Charitable Fund, and B. W.-K. C. the receipt of a postdoctoral fellowship supported by the AoE on Institute of Molecular Technology of the UGC and the Generic Drug Research Program of The University of Hong Kong. The work described in this paper has been supported by the Research Grants Council of the Hong Kong Special Administrative Region, China (Project HKU7140/99P).

References

1 (*a*) J. P. Paris and W. W. Brandt, *J. Am. Chem. Soc.*, 1959, **81**, 5001; (*b*) J. N. Demas and A. W. Adamson, *J. Am. Chem. Soc.*, 1971, **93**, 1800; (*c*) J. N. Demas and A. W. Adamson, *J. Am. Chem. Soc.*, 1972, **94**, 8238; (*d*) V. Balzani, F. Bolleta, M. T. Gandolfi and M. Maestri, *Top. Curr. Chem.*, 1978, **75**, 1; (*e*) N. Sutin, *J. Photochem.*, 1979, **10**, 19; (*f*) N. Sutin and C. Creutz, *Pure Appl. Chem.*, 1980, **52**, 2717; (*g*) K. Kalyanasundaram, *Coord. Chem. Rev.*, 1982, **46**, 159; (*h*) A. Juris, V. Balzani, F. Barigelletti, S. Camagna, P. Belser and A. zon Zelwewsky, *Coord. Chem. Rev.*, 1988, **84**, 85; (*i*) R. J. Watts, *J. Chem. Educ.*, 1983, **60**, 835; (*j*) E. A. Seddon and K. R. Seddon in *The Chemistry of Ruthenium*, Elsevier, Amsterdam, 1984; (*k*) R. A. Krause, *In Structure and Bonding*, 1987, **67**, 1.

2 (*a*) V. W. W. Yam, B. W. K. Chu and K. K. Cheung, *Chem. Commun.*, 1998, 2261; (*b*) V. W. W. Yam, B. W. K. Chu, C. C. Ko and K. K. Cheung, *J. Chem. Soc., Dalton Trans.*, 2001, 1911; (*c*) T. Tomon, D. Ooyama, T. Wada, K. Shiren and K. Tanaka, *Chem. Commun.*, 2001, 1100.

3 (*a*) R. H. Grubbs, in *Comprehensive Organometallic Chemistry*, Pergamon, New York, 1982, vol. 8, p. 499; and references therein; (*b*) R. H. Grubbs, S. J. Miller and G. C. Fu, *Acc. Chem. Res.*, 1995, **28**, 446 and references therein; (*c*) T. M. Trnka and R. H. Grubbs, *Acc. Chem. Res.*, 2001, **34**, 18 and references therein.

4 See, for example: (*a*) Y. Degani and I. Willner, *J. Chem. Soc., Chem. Commun.*, 1985, 648; (*b*) A. M. Echavarren, J. Lopez, A. Santos, A. Romero, J. A. Hermoso and A. Vegas, *Organometallics*, 1991, **10**, 2371; (*c*) J. Montoya, A. Santos, J. Lopez, A. M. Echavarren, J. Ros and A. Romero, *J. Organomet. Chem.*, 1992, **426**, 383; (*d*) T. Rappert and A. Yamamoto, *Organometallics*, 1994, **13**, 4984; (*e*) M. A. Esteruelas, A. Miguel, F. J. Lahoz, A. M. Lopez, E. Onate and L. A. Oro, *Organometallics*, 1994, **13**, 1669; (*f*) H. Nishiyama, Y. Itoh, H. Matsumoto, S. B. Park and K. Itoh, *J. Am. Chem. Soc.*, 1994, **116**, 2223; (*g*) S. B. Park, H. Nishiyama, Y. Itoh and K. Itoh, *J. Chem. Soc., Chem. Commun.*, 1994, 1315; (*h*) A. Pedersen, M. Tilset, K. Folting and K. G. Caulton, *Organometallics*, 1995, **14**, 875; (*i*) C. M. Che, S. M. Yang, M. C. W. Chan, K. K. Cheung and S. M. Peng, *Organometallics*, 1997, **16**, 2819; (*j*) Y. Zhu, O. Clot, M. O. Wolf and G. P. A. Yap, *J. Am. Chem. Soc.*, 1998, **120**, 1812; (*k*) A. Klose, E. Solari, C. Floriani, S. Geremia and L. Randaccio, *Angew. Chem., Int. Ed. Engl.*, 1998, **37**, 148.
5 J. Hassan, V. Penalva, L. Lavenot, C. Gozzi and M. Lemaire, *Tetrahedron*, 1998, **54**, 13793.
6 K. Kikukawa, G. X. He, A. Abe, T. Goto, R. Arata, T. Ikeda, F. Wada and T. Matsuda, *J. Chem. Soc., Perkin Trans 2*, 1987, 135.
7 S. Takahashi, Y. Kuroyama, Y. Sonogashira and N. Hagihara, *Synthesis*, 1980, 627.
8 B. P. Sullivan, D. J. Salmon and T. J. Meyer, *Inorg. Chem.*, 1978, **17**, 3334.
9 J. Bourson, J. Pouget and B. Valeur, *J. Phys. Chem.*, 1993, **97**, 4552.
10 DENZO (version 1.3.0): *The HKL Manual – A description of programs DENZO, XDISPLAYF and SCALEPACK*, written by D. Gewirth with the cooperation of the program authors Z. Otwinowski and W. Minor, 1995, Yale University, New Haven, USA.
11 A. Altomare, M. C. Burla, M. Camalli, G. Cascarano, C. Giacovazzo, A. Guagliardi, A. G. G. Moliterni, G. Polidori and R. Spagna, *J. Appl. Crystallogr.*, 1998, **32**, 115.
12 G. M. Sheldrick, SHELXS-97, SHELX-97, Programs for Crystal Structure Analysis (Release 97–2), University of Göttingen, Germany, 1997.
13 P. B. Hitchcock, M. F. Lappert and P. L. Pye, *J. Chem. Soc., Dalton Trans.*, 1978, 826.
14 D. Schomburg, S. Neumann and R. Schmutzler, *J. Chem. Soc., Chem. Commun.*, 1979, 848.
15 F. A. Cotton and C. M. Lukehart, *Prog. Inorg. Chem.*, 1972, **16**, 487.
16 (*a*) G. A. Crosby, *Acc. Chem. Res.*, 1975, **8**, 231; (*b*) P. G. Bradley, N. Kress, B. A. Hornberger, R. F. Dallinger and W. H. Woodruff, *J. Am. Chem. Soc.*, 1981, **103**, 7441; (*c*) E. M. Kober, B. P. Sullivan, W. J. Dressick, J. V. Caspar and T. J. Meyer, *J. Am. Chem. Soc.*, 1980, **102**, 7383; (*d*) J. V. Caspar, E. M. Kober, B. P. Sullivan and T. J. Meyer, *J. Am. Chem. Soc.*, 1982, **104**, 630; (*e*) J. V. Caspar and T. J. Meyer, *Inorg. Chem.*, 1983, **22**, 2444.
17 (*a*) J. N. Demas and G. A. Crosby, *J. Am. Chem. Soc.*, 1971, **93**, 2841; (*b*) A. J. Juris, V. Balzani, P. Belser and A. von Zelewsky, *Helv. Chim. Acta*, 1981, **64**, 2175; (*c*) K. Kalyanasundaram, *Coord. Chem. Rev.*, 1982, **46**, 159 and references therein.
18 (*a*) H. K. Frensdorff, *J. Am. Chem. Soc.*, 1971, **93**, 600; (*b*) J. J. Christensen, D. J. Eatough and R. M. Izatt, *Chem. Rev.*, 1974, **74**, 351; (*c*) R. M. Izatt, K. Pawlak, J. S. Bradshaw and R. L. Bruening, *Chem. Rev.*, 1991, **91**, 1721.